Negative Correlations Between Cultivable Pyrene-degrading Sphingomonas and Active Soil Pyrene Degraders Explain Bioaugmentation Postpone or Failure

Bo Jiang
University of Science and Technology Beijing
Yating Chen
University of Science and Technology Beijing
Yi Xing
University of Science and Technology Beijing
Luning Lian
University of Science and Technology Beijing
Yaoxin Shen
University of Science and Technology Beijing
Baogang Zhang
China University of Geosciences Beijing
Han Zhang
China University of Geosciences Beijing
Guangdong Sun
Tsinghua University
Junyi Li
Yiqing (Suzhou) Environmental Technology Co. Ltd.
Xinzi Wang
Tsinghua University
Dayi Zhang (zhangdayi@tsinghua.edu.cn)
Tsinghua University https://orcid.org/0000-0002-1647-0408

Research

Keywords: Bioaugmentation, pyrene, soils, magnetic nanoparticle-mediated isolation (MMI), degradation pathway

Posted Date: May 27th, 2021

DOI: https://doi.org/10.21203/rs.3.rs-553986/v1

Abstract

Background: Bioaugmentation is an effective approach to remediate soils contaminated by polycyclic aromatic hydrocarbon (PAHs), but suffers from unsatisfactory performance in engineering practices. It is hypothetically explained by the complicated interactions between indigenous microbes and introduced degrading consortium. This study isolated a cultivable pyrene degrader (*Sphingomonas sp.* YT1005) and an active pyrene degrading consortium consisting of *Gp16*, *Streptomyces*, *Pseudonocardia*, *Panacagrimonas*, *Methylotenera* and *Nitrospira* by magnetic-nanoparticle mediated isolation (MMI) from soils.

Results: Pyrene biodegradation was postponed in bioaugmentation with *Sphingomonas sp.* YT1005, explained by its negative correlations with the active pyrene degraders. In contrast, amendment with the active pyrene degrading consortium, pyrene degradation efficiency increased by 30.17%. In addition, pyrene degradation efficiency was positively correlated with the abundance of pyrene dioxygenase encoding genes (*nidA*, *nidA3* and PAH-RHDα-GP), which significantly increased in MMI-isolated consortium. Pyrene degradation by *Sphingomonas sp.* YT1005 only followed the phthalate pathway, whereas the MMI-isolated pyrene degrading consortium exhibited both phthalate and salicylate pathways. The results indicated that *Sphingomonas sp.* YT1005 was not the actual pyrene degrader in soils, and MMI could successfully isolate the active pyrene degraders that were suitable for bioaugmentation.

Conclusion: This work revealed the microbial intra-correlations during the bioaugmentation process, uncovered the underlying mechanisms of bioaugmentation postpone with cultivable degraders, and provided a deeper insight into the actual pyrene degraders and degradation pathways in PAHs contaminated soils. Our findings gave new explanations for bioaugmentation postpone or failure, and offered clues to enhance bioaugmentation performance by the active degraders using MMI.

1. Introduction

Polycyclic aromatic hydrocarbons (PAHs) are a typical group of persistent organic pollutants (POPs) containing two or more combined aromatic rings in linear, angular or cluster arrangements (Ghosal et al 2016). As natural constituents in fossil fuels, PAHs are present with high concentrations at sites with petroleum refining and transportation activities (Kanaly and Harayama 2000). At least 600 of 1,408 most severely contaminated sites in USA are contaminated with PAHs (Duan et al 2015). Additionally, PAHs can migrate into soils through dry and wet atmospheric deposition (Wang et al 2017a, Nam et al 2008), and soils are able to attenuate PAHs transport and eventually serve as major sinks (Liu et al 2019, Okere et al 2017). The average $\sum$16-PAHs in Orlando and Tampa soils are 3.23 and 4.56 mg/kg, respectively, mainly attributing to vehicle emissions and combustion of biomass or coals (Liu et al 2019). Moreover, soil PAHs can enter the food chain through bioaccumulation, imposing serious threats to human health due to their teratogenic, carcinogenic and mutagenic properties (Wang et al 2017b, Kim et al 2013). Thus,

PAHs have gained great attentions in recent decades for their ubiquitous presence in environment and high resistance to degradation.

Bioremediation is known as a cost-efficient and environmentally friendly approach to degrade soil pollutants, exhibiting low risks in secondary pollution (Peng et al 2008, Haleyur et al 2018). PAH-degrading bacteria are capable of metabolizing various PAHs *via* enzymatic attacks on different carbon positions due to the broad substrate specificity and regiospecificity of dioxygenase (Zeng et al 2017, Segura et al 2017). PAH ring hydroxylating dioxygenase (PAH-RHD) are responsible for the initial step of PAHs metabolism (Cebron et al 2008), and the encoding genes include *ahd* (Pinyakong et al 2003), *dox* (Denome et al 1993), *flnA1/ A2* (Schuler et al 2008), *nag* (Izmalkova et al 2013), *nahR* (Bosch et al 2000), *nar* (Liu et al 2011), *nidA/ B* (Stingley et al 2004), *nidA3* (Chen et al 2016), *pah* (Takizawa et al 1999), *pdo* (Krivobok et al 2003), *phd* (Saito et al 1999) and *phn* (Izmalkova et al 2013). Particularly, pyrene is a typical PAH for its similar structure to several carcinogenic PAHs (Peng et al 2008) and its biodegradation has been intensively studied *via* either metabolism as carbon and energy source, or co-metabolism as a non-growth substrate (Johnsen et al 2005, Nzila 2013). Pyrene degraders include *Acinetobacter* (Jiang et al 2018a), *Burkholderia* (Vaidya et al 2017), *Bacillu*s (Rabodonirina et al 2018), *Mycobacterium* (Wu et al 2019), *Pseudomonas* (Khan et al 2018), *Rhodococcus* (Jia et al 2019) and *Sphingomonas* (Guo et al 2017). Genes encoding pyrene dioxygenase include *nidA* and *nidA3* (Cebron et al 2008, Zhou et al 2006).

Bioaugmentation is a practical strategy to improve bioremediation performance at contaminated sites by introducing competent strains or consortia capable of degrading target contaminants (Perelo 2010). For instance, bioaugmentation with autochthonous *Acinetobacter tandoii* LJ-5 significantly improved phenanthrene removal efficiency by changing the diversity of phenanthrene degraders (Li et al 2018). Other stains for successful bioaugmentation include *Klebsiella pneumonia* capable of degrading naphthalene, anthracene, acenaphthene and fluorene (Mohanrasu et al 2018) and *Acinetobacter johnsonii* co-biodegrading pyrene, phenanthrene, naphthalene and anthracene (Jiang et al 2018a). Although several field studies have demonstrated the feasibility of bioaugmentation to enhance bioremediation performance in groundwater (Major et al 2002), wastewater (Wu et al 2018) and aquifer (Dybas et al 2002), scaling up from laboratory to commercial-scale field is always a challenge. Both abiotic (temperature, moisture, pH, organic matter, aeration, nutrient and soil type) (Heinaru et al 2005) and biotic factors (competition between indigenous and exogenous microorganisms for limited nutrients) (Sørensen et al 1999, Mrozik and Piotrowska-Seget 2010) play essential roles in bioaugmentation performance. Additionally, the mechanisms of bioaugmentation are argued recently (Thompson et al 2005), and little is known about the interactions of the re-introduced degraders with indigenous microbes during bioaugmentation process.

Although cultivation-dependent approaches have isolated many PAH degraders, less than 1% of soil microorganisms are cultivable under artificial conditions (Kaeberlein et al 2002, Vartoukian et al 2010). Stable isotope probing (SIP) is a well-developed approach to identify functional-yet-uncultivable PAH degraders *in situ* (Jiang et al 2018b). However, SIP relies on the isotope incorporation in the active degraders, *e.g.*, DNA, RNA and proteins. More importantly, SIP cannot isolate the living degraders and is

not suitable to provide bioaugmentation strains for practices. Recently, a novel technique, magnetic-nanoparticle mediated isolation (MMI), is innovated and aims at separating the active degraders from inert bacteria by magnetic gradient (Zhang et al 2015, Zhao et al 2016). This isotope-independent approach can isolate the active degraders from complex environment in a cost-effective manner and the separated microbes remain viable to be used in bioaugmentation (Sun et al 2021).

In the present study, both cultivation-dependent and MMI approaches were applied to isolate pyrene degraders from pyrene-contaminated soils at an abandoned steel plant site. Using cultivable pyrene degrader *Sphingomonas sp.* YT1005 and MMI-enriched active pyrene-degrading consortium in bioaugmentation, we analyzed the pyrene degradation efficiency, metabolic pathway, bacterial community structure and pyrene dioxygenase encoding genes. This work attempted to unravel the active pyrene degraders in soils, explore suitable inoculates in bioaugmentation for enhanced pyrene degradation, understand the bacterial interactions during bioaugmentation process, and explain the restriction factors causing bioaugmentation postpone or failure. As the first study to separate and introduce the active pyrene-degrading microbes in soil bioaugmentation, this work can broaden our knowledge on the influential factors affecting bioaugmentation performance and provide an effective approach isolating and applying the active degraders to improve bioaugmentation performance at PAHs-contaminated sites.

2. Materials And Methods

2.1. Soil sample collection and analysis

Soil samples were collected at an abandoned site of Capital Steel Plant located in Shijingshan District, Beijing. This site was severely contaminated by PAHs and the PAHs concentration ranged from several to over 500 mg/kg. One kilogram of soils were obtained from the surface layer (0–20 cm) in the absence of PAHs contamination, stored at 4ºC and transferred to laboratory. After homogenization, stones and plant debris were removed. Soil geochemical properties were analyzed and listed in Table S1 (Electronic Supporting Information, ESI). There was no detectable PAHs in the collected soils.

2.2. Magnetic nanoparticle synthesis and functionalization

The synthesis of magnetic nanoparticles (MNPs) followed our published method (Zhang et al 2011). Briefly, 1 mL of $FeCl_2$ (1 mol/L in 2.0 M of HCl) and 2 mL of $FeCl_3$ (2 mol/L in 2.0 M of HCl) were gently mixed. Afterwards, 25 mL of NaOH (2 mol/L) was added drop by drop with vortex constant mixing for 30 min. The synthesized dark nanoparticles were then harvested by an external magnet for 10 min and washed with 30 mL of deionized water for several times until pH was neutral. The concentration of synthesized MNPs was 9.1 g/L. According to the optimal dosage for soil magnetic functionalization (Wang et al 2016), 0.91 mg of synthesized MNPs (0.1 mL) were added to 500 mg soils (dry weight) to prepare MNP-functionalized soils to isolate the active pyrene degrading consortium.

2.3. Isolation of cultivable pyrene degraders

Four grams of original soils were added into 100 mL of enrichment medium supplemented with pyrene (100 mg/L). The enrichment medium contained 5 g of beef extract, 10 g of peptone, 5 g of NaCl, 0.5 g of NaH_2PO_4 and 1.5 g of Na_2HPO_4 in 1.0 L of deionized water. After 7-day incubation with continuous shaking (180 rpm) at 28ºC in the dark, 1 mL of the suspension was transferred into 100 mL of fresh enrichment medium with increasing pyrene concentration (200, 300, 400 and 500 mg/L). Afterwards, the enriched suspension was diluted and spread onto a mineral medium agar plate supplemented with pyrene (500 mg/L) as the sole carbon source. One litre of mineral medium contained 0.5 g of KH_2PO_4, 0.5 g of NaCl, 0.1 g of $CaCl_2$, 0.2 g of $MgSO_4 \cdot 7H_2O$, 0.5 g of $FeSO_4 \cdot 7H_2O$, 0.5 g of $MnSO_4$ and 1.5 g of $(NH_4)_2SO_4$ (Zhang et al 2012). After incubation at 28ºC for 2 days in the dark, single colonies were picked from the plate and spread twice on fresh mineral medium agar plates supplemented with pyrene (500 mg/L) for purification.

The 16S rRNA genes of the isolated pyrene degraders were amplified by polymerase chain reaction (PCR) with a primer pair of 27F (5'-AGAGTTTGATCCTGGCTCAG-3') and 1492R (5'-GCTACCTTGTTACGACTT-3') (Guo et al 2010). PCR amplification consisted of 1 cycle of 95ºC for 5 min, 35 cycles of 95ºC for 30 s, 56ºC for 30 s and 72ºC for 1 min, and a final extension at 72ºC for 10 min. The purified PCR products were used for sequence, and sequence similarity searches and alignments were performed using BLASTN at http://www.ncbi.nlm.nih.gov/BLAST/. All isolates have identical sequence sharing 98% similarity with *Sphingomonas echinoides* strain DSM 1805 (NCBI Accession No. MK934417), named as *Sphingomonas sp.* YT1005.

2.4. Pyrene degradation microcosms

To explore pyrene biodegradation performance in soils, five treatments were carried out as follows: original soils treated with $HgCl_2$ (0.1%) and supplemented with pyrene as sterile control (OS_CK), original soils without pyrene (OS_NC), original soils supplemented with pyrene (OS_Pyr), MNP-functionalized soils without pyrene (MMI_NC) and MNP-functionalized soils supplemented with pyrene (MMI_Pyr). For OS_CK, OS_Pyr and MMI_Pyr treatments, pyrene was set at a final concentration of 100 mg/kg, meeting with the average contamination level at the contaminated site. Each treatment was conducted in triplicates and incubated at room temperature for 30 days. After 0, 10, 20 and 30 days of cultivation, 5.0 g of soil samples were collected for chemical analysis and DNA extraction. To separate the active pyrene degrading consortium (magnetic-free cells, MFCs), 2.0 g of soils were collected from MMI_NC and MMI_Pyr treatments on Day 0, 10, 20 and 30. Subsequently, the soils were added with 3 mL of soil extraction solution (2.0 g of original soils with 20 mL deionized water and passing through a 0.45-mm filter) and further separated by a permanent magnet (Wang et al 2016). MFCs in suspensions separated from MMI_NC and MMI_Pyr treatment were designated as MFC_NC and MFC_Pyr.

Bioaugmentation experiment introduced the cultivable pyrene degrader *Sphingomonas sp.* YT1005 or MFCs (MMI-enriched pyrene-degrading consortium) into soils with total populations of 10^9 cells/g soil. The four treatments included: original soils supplemented with *Sphingomonas sp.* YT1005 (BA_Sph), sterile soils supplemented with *Sphingomonas sp.* YT1005 (CK_Sph), original soils supplemented with

MFCs (BA_MFC), and sterile soils supplemented with MFCs (CK_MFC). Pyrene was set at a final concentration of 100 mg/kg in all treatments, which were incubated at 28ºC in the dark in triplicates. Finally, 5.0 g of soils were sacrificed after 0, 10 and 20 days for chemical analysis and DNA extraction.

2.5. DNA extraction and quantification of PAHs-degrading genes

Soil genomic DNA was extracted from all soil samples using a MO BIO PowerSoil DNA Isolation Kit (MoBio Laboratories, Inc., USA) according to the manufacturer's instructions. DNA concentration was determined by spectrophotometry (NanoDrop 2000, Wilmington, DE). Quantitative PCR (qPCR) was performed for the abundance of bacterial 16S rRNA and pyrene dioxygenase encoding genes, including PAH-RHDα-GP, PAH-RHDα-GN, *nidA* and *nidA3*. PCR primer pairs were listed in Table S2 (ESI) and PCR program was set as follows: an initial denaturation at 95ºC for 5 min, followed by 35 cycles of 95ºC denaturation for 30 s, annealing at different temperatures for each primer set (Table S2) for 30 s and extension at 72ºC for 1 min, and a final extension at 72ºC for 10 min. The standard curves of C*t* value and copy numbers for each gene were obtained by generating a ten-fold serial dilution of plasmids containing corresponding genes. The relative abundance of pyrene dioxygenase encoding genes was calculated as the ratio of the copy numbers of pyrene dioxygenase encoding genes to those of 16S rRNA genes.

2.6. Bacterial community analysis

To assess bacterial community composition and diversity in each treatment, the extracted DNA was amplified and sequenced targeting the V3-V4 regions of 16S rRNA genes (Sangon Biotech Co., Ltd, Beijing, China). PCR was performed using the universal primer set of 515F (5'-GTGCCAGCMGCCGCGGTAA-3') and 806R (5'-GGACTACHVGGGTWTCTAAT-3') (Song et al 2015). The 806R primer was labeled with a unique 6-bp barcode to distinguish amplification products. Sequencing was performed by Illumina Miseq™ and all sequence reads were quality checked after removing primer connector sequences, merging paired reads and distinguishing samples according to barcodes (NCBI BioProject ID: PRJNA534380). Sequences were classified as operational taxonomic units (OTUs) with 97% similarity and then assigned by Ribosomal Database Project (RDP) classifier based on Bergey's taxonomy. Bacterial alpha-diversity indices (Chao1, Shannon and Simpson) was analyzed by QIIME (v1.80) to assess bacterial species richness and diversity. Bacterial beta-diversity distance matrices among samples were generated via Bray-Curtis dissimilarity by FastTree (http://www.microbesonline.org/fasttree) and Fastunifrac (http://unifrac.colorado.edu) software (Hamady et al 2010).

2.7. Chemical analysis

To analyze soil pyrene contents, 5.0 g of soils were blended with 3 g of anhydrous Na_2SO_4, spiked with 10 μg of surrogate standards (phenanthrene-d10, AccuStandard®, Inc.), and added with 15 mL of extraction solvent (hexane:acetone = 1:1, v/v). After ultrasonication-assisted extraction for 20 min, the suspension was centrifuged for 3 min at 10,000 rpm. The extraction process was repeated twice, and the

three fractions of supernatants were mixed and concentrated using a rotary evaporator to a final volume of approximately 2 mL. It was further purified by solid phase extraction cartridges which were pre-conditioned with 4 mL of dichloromethane and 10 mL of hexane, and washed by 5 mL of dichloromethane:hexane (1:9, v/v). After soaking for 2 min, another 5 mL of dichloromethane:hexane (1:9, v/v) were added to elute pyrene and the filtrates were concentrated to completely dry under a gentle stream of nitrogen gas. Internal standards (fluorene, 100 μg/mL) were added to each filtrate prior to instrumental analysis.

The quantitative analysis of pyrene was performed using a gas chromatography mass spectrometry (GC-MS, Shimadzu, QP2010SE) equipped with a DB-5MS capillary column (30 m in length, 0.25 mm in diameter, 0.25 μm thickness) and a mass spectrometric detector. A total of 1.0 μL sample was injected in the splitless mode with a 5-min solvent delay time. The carrier gas was helium (99%) at a rate of 1.0 mL/min and the injector temperature was 280ºC. The GC oven temperature was set at 80ºC for 2 min, raised to 180ºC at a rate of 20ºC/min and maintained at 180 ºC for 5 min, and finally raised to 290ºC at a rate of 10ºC/min and maintained at 290ºC for 5 min. Electron impact source and selected ion monitoring (SIM) mode were used to identify individual metabolite. The ion source temperature was 230℃ and scanning range was from 45 to 450 atomic mass units (amu).

Five pyrene standard concentrations (5-500 μg/mL) were used to derive the calibration curve for pyrene. Mean recoveries of surrogate standards (phenanthrene-d10) in the present study ranged from 90–105% and the final concentrations of pyrene were corrected by surrogate recovery. For pyrene metabolites, the molecular mass of each metabolite was searched against previous literatures and the database of PAH metabolites (National Institute of Standards and Technology, NIST). The chemical structure of each possible metabolite was confirmed by the pattern of fragment ions in the mass spectrum.

2.8. Statistical analysis

Statistical analysis was performed by SPSS 20.0 software. One-way analysis of variance (ANOVA) was used to compare the difference in pyrene contents and the relative abundance of 16S rRNA and pyrene dioxygenase encoding genes ($p < 0.05$). The correlation matrix was calculated and visualized using R (version 3.5.3). The phylogenetic tree of 16S rRNA genes was constructed according to the neighbor joining method using Molecular Evolutionary Genetics Analysis (MEGA). Molecular ecological network was constructed by online MENA (Molecular Ecological Network Analyses) pipeline (http://ieg2.ou.edu/MENA) using Spearman's Rho with default parameters (Deng et al 2018).

The logarithmic nonlinear regression between pyrene degradation efficiency (P_D, %) and the abundance of pyrene dioxygenase encoding genes ($Pyrene_g$, copies/g soil) followed Eq. (1):

$$P_D = P_0 + a \times \ln (Pyrene_g) \qquad (1)$$

Here, P_0 and α represents pyrene degradation efficiency in abiotic treatments and correlation slope, respectively.

3. Results

3.1. Biodegradation and bioaugmentation performance

Pyrene degradation efficiencies in different treatments are illustrated in Fig. 1. In abiotic treatment (NC_Pyr), pyrene content did not show significant decrease throughout the incubation period. An acceptable pyrene degradation was achieved in OS_Pyr treatment, and pyrene degradation efficiency was 30.18% on day 10 and 44.24% on day 20.

After introducing the cultivable pyrene degraders (*Sphingomonas sp.* YT1005 in BA_Sph and CK_Sph treatments and MMI-isolated active pyrene-degrading consortium in BA_MFC and CK_MFC treatments) in bioaugmentation, pyrene degradation performance varied remarkably across treatments (Fig. 1). An unexpected postpone of pyrene degradation was found in BA_Sph and CK_Sph treatments that pyrene degradation efficiency was less than 20% after 20-day incubation, exhibiting no significant difference with that in abiotic sterile treatment (OS_CK, $p > 0.05$). BA_MFC treatment (original soils with MMI-isolated active pyrene-degrading consortium) accelerated pyrene degradation efficiency to 57.79% on day 10 and 74.41% on day 20. It is worth highlighting that CK_MFC treatment (sterile soils with MMI-isolated active pyrene-degrading consortium) had a similar pyrene degradation curve as OS_Pyr treatment, suggesting that the introduced active pyrene-degrading consortium alone had the same pyrene degradation capabilities as indigenous soil microbes.

3.2. Microbial community diversity and structure during pyrene degradation process

After processing raw data obtained by Illumina Miseq, a total of 895,290 raw reads with a length of > 450 bp were obtained from 19 soil samples in five treatments, ranging from 50,899 in MMI_Pyr_30 to 77,369 in MMI_Pyr_20. They were assigned into 15,210 OTUs affiliated with 30 bacterial phyla and 100 bacterial genera. Across all samples, the Good's coverage ranged from 0.95 to 0.99, indicating a satisfactory coverage of bacterial lineages for further analysis. In all treatments, bacterial alpha-diversity indices (Chao1, Shannon and Simpson) did not show significant difference (Table S3).

Sphingomonas was the most predominant bacterial genus, accounting for 4.12% of total bacterial populations in treatment without pyrene (OS_NC) to 37.81% in MFC_Pyr treatments. Other dominant bacterial genera included *Arthrobacter* (9.33–9.87%), *Lysobacter* (3.42–6.24%), *Rhodococcus* (3.07–5.19%), *Pedobacter* (3.43–4.06%), *Aeromicrobium* (3.00–3.07%) and *Pseudonocardia* (2.47–3.58%) in original soils and OS_NC treatments (Figure S1).

From bacterial beta-diversity distance matrices (Fig. 2A), bacterial community compositions in OS_NC and OS_Pyr treatments were similar and clustered together in the first 10-day of pyrene degradation. Afterwards, the relative abundance of some bacterial taxa in OS_Pyr treatments was significantly higher than that in OS_NC treatments, including *Kribbella* (2.00%), *Streptomyces* (2.92%), *Lysobacter* (8.69%), *Streptomyces* (4.75%) and *Thermomonas* (3.24%). Accordingly, the groups of OS_NC and OS_Pyr were

separated after day 10. Similarly, bacterial communities in MMI_NC and MMI_Pyr treatments were also clustered (Fig. 2A). In the absence of pyrene, bacterial community composition showed no difference between MMI_NC and MFC_NC (Fig. 2B).

3.3. Pyrene degraders revealed by cultivation-dependent and cultivation-independent methods

In total, 8 isolates were obtained from mineral medium agar plates supplemented with pyrene. The results of 16S rRNA gene sequencing demonstrated that all isolates have identical sequence, exhibiting 98% similarity with *Sphingomonas echinoides* strain DSM 1805 (NCBI Accession No: MK934417). This cultivable pyrene degrader was then designated as *Sphingomonas sp.* YT1005. With pyrene as the sole carbon source, this strain formed orange pigmented colonies on agar plates. Additionally, *Sphingomonas sp.* YT1005 had a satisfactory pyrene degradation efficiency, which achieved 62.3% after 10-day incubation in mineral medium.

In MMI_Pyr treatment, as the active pyrene degraders could utilize pyrene and proliferate, they gradually lose their magnetism and were separated by external magnetic field. Bacterial beta-diversity distance matrices illustrated that MFCs isolated from MMI_Pyr treatment (MFC_Pyr) were separated from the whole community in MMI_Pyr treatment and MFC_NC (MFCs from MMI_NC treatments, Fig. 2B). Accordingly, by comparing the relative abundance of bacterial lineages, several bacterial genera were much higher in MFC_Pyr and they were potentially the active pyrene degraders. They included *Gp16*, *Streptomyces*, *Pseudonocardia*, *Panacagrimonas*, *Methylotenera* and *Nitrospira*, which was 1.442 ± 0.207, 1.511 ± 0.216, 1.621 ± 0.615, 4.573 ± 1.641, 2.526 ± 0.698 and 1.533 ± 0.052 times more enriched in MFC_Pyr, respectively (Fig. 2C).

In treatments without pyrene (OS_NC), neither *Sphingomonas sp.* YT1005 nor the active pyrene degrading consortium (*Gp16*, *Streptomyces*, *Pseudonocardia*, *Panacagrimonas*, *Methylotenera* and *Nitrospira*) were enriched in the magnetic-free fraction (MFC_NC, Fig. 3A), remaining 28.0-30.6% and 1.9-3.0% throughout the pyrene degradation process, respectively. In contrast, the relative abundance of *Sphingomonas sp.* YT1005 in MFC_Pyr fraction significantly decreased from 26.5–8.5%, whereas the relative abundance of potential pyrene degraders increased from 2.3–5.2% (Fig. 3B). These results proved that *Sphingomonas sp.* YT1005 was not active pyrene degraders, and the increasing populations of the potential active pyrene degraders contributed to the enhanced pyrene degradation performance in bioaugmentation.

The phylogenetic tree of the cultivable pyrene degrader *Sphingomonas sp.* YT1005 and the potential active pyrene degraders in MFC_Pyr is illustrated in Fig. 3C. *Sphingomonas sp.* YT1005 is clustered with other *Sphingomonas* species, e.g., *Sphingomonas echinoides* and *Sphingomonas glacialis*. All the potential active pyrene degraders isolated from MMI_Pyr treatment, including *Nitrospira* (OTU23472), *Gp16* (OTU33542), *Streptomyces* (OTU29458), *Pseudonocardia* (OTU29851), *Panacagrimonas* (OTU4395) and *Methylotenera* (OTU583), were clustered in a separate branch.

3.4. Intra-correlation within soil bacterial community

To explain the mechanisms of bioaugmentation postpone in BA_Sph and CK_Sph treatments, we analyzed the bacterial intra-correlations by molecular ecological network (Fig. 4, Table S4). The results suggested a complex microbial network in soils (avgK = 4.356 and avgCC = 0.205), including 4 major modules, 360 nodes and 784 significant correlations ($p < 0.01$). The majority (90.1%) of the correlations were positive, and the cultivable pyrene degrader *Sphingomonas* (OTU33525) exhibited 12 positive links with Module 2. Four of the potential active pyrene degraders (*Nitrospira*, OTU23472; *Streptomyces*, OTU29458; *Panacagrimonas*, OTU4395; *Methylotenera* OTU583) had 39 correlations with other bacterial lineages, 56.4% of which were negative. It is worth noting that, although there was no direct correlation between the cultivable pyrene degrader *Sphingomonas* and the potential active pyrene degraders, 11 indirect correlations (mediated by other microbes from the 4 major modules) were observed and they were all negative. Additionally, Mantel test confirmed the negative correlations between *Sphingomonas* and the potential active pyrene degraders ($p < 0.05$), and the correlation coefficient was − 0.7285 for *Gp16*, -0.7533 for *Streptomyces*, -0.8287 for *Pseudonocardia*, -0.7548 for *Panacagrimonas* and − 0.7956 for *Methylotenera* ($p < 0.05$). Our results therefore uncovered negative correlations between the cultivable pyrene degrader *Sphingomonas sp.* YT1005 and the active pyrene degrading consortium isolated by MMI, which suppressed the bioaugmentation performance in BA_Sph and CK_Sph treatments.

3.5. Dynamics of pyrene dioxygenase encoding genes

No PAH-RHDα-GN gene was successfully amplified in any treatment. The relative abundance of *nidA*, *nidA3* and PAH-RHDα-GP genes in OS_NC treatment remained constant throughout the incubation period (Fig. 5A), ranging from 0.96×10^{-7} to 1.32×10^{-7}, 3.62×10^{-7} to 4.25×10^{-7} and 44.5×10^{-7} to 50.1×10^{-7}, respectively. It indicated a neglectable increase of pyrene dioxygenase encoding genes in the absence of pyrene. The relative abundance of *nidA*, *nidA3* and PAH-RHDα-GP genes increased significantly ($p < 0.01$) in OS_Pyr treatments since day 20 and finally achieved 1.00×10^{-5}, 2.84×10^{-5} and 2.15×10^{-5} on day 30, which was 105.5, 74.6 and 4.7 times higher than those in OS_NC treatments. Interestingly, all these pyrene dioxygenase encoding genes dramatically increased in MFC_Pyr from day 10. After 30-day degradation, the relative abundance of *nidA*, *nidA3* and PAH-RHDα-GP genes increased to 1.13×10^{-4}, 2.88×10^{-4} and 2.24×10^{-4}, which was 1182.6, 754.8 and 49.3 times higher than that in OS_NC treatments.

There were significantly positive correlations between pyrene degradation efficiency and the relative abundance of *nidA*, *nidA3* and PAH-RHDα-GP genes ($p < 0.01$, Table 1). The regression coefficient was 2.72×10^{-6} ($r^2 = 0.9671$), 4.74×10^{-6} ($r^2 = 0.9064$) and 1.60×10^{-6} ($r^2 = 0.8790$) for *nidA*, *nidA3* and PAH-RHDα GP genes, respectively (Fig. 5B).

Table 1
Spearman rank correlation coefficient (r_s) matrix.

	Pyrene degradation efficiency	*nidA*	*nidA3*	GP
Pyrene degradation efficiency	-			
nidA	0.98**	-		
nidA3	0.98**	0.99**	-	
PAH-RHDα GP	0.99**	0.99**	0.99**	-
Significant correlations are marked with asterisks ($p < 0.01$, n = 6).				

3.6. Metabolites and degradation pathway of pyrene

To understand pyrene degradation pathways in bioaugmentation, metabolites were analyzed during pyrene biodegradation process in CK_Sph and CK_MFC treatments. In total, ten metabolites were identified, and two pyrene degradation pathways were proposed (Fig. 6 and S3, Table S3).

In CK_Sph treatment, the metabolite *cis*-4,5-pyrene dihydrodiol (m/z = 364, t_R=19.82 min) might be generated from an initial pyrene oxidation at C-4 and C-5 positions by dioxygenase, designated as metabolite ⓐ. Although the following metabolite phenanthrene-4-carboxylic acid (by *ortho*-cleavage and decarboxylation) was not detectable, its downstream metabolite was detected as dihydroxyphenanthrene (metabolite ⓑ, m/z = 355, t_R=5.31 min). Further oxidation of dihydroxyphenanthrene generated 2-hydroxy-2-H-benzo[h]chromene-2-carboxylic acid (metabolite ⓒ, m/z = 415) by extradiol dioxygenase after ring cleavage, and subsequent to 2-methylnaphthalene (metabolite ⓓ, m/z = 142) and 1-hydroxy-2-naphthoic acid (metabolite ⓔ, m/z = 202). Finally, metabolite ⓕ (m/z = 167, t_R=21.73 min) was identified as phthalic acid comparing to the mass spectral library (NIST). From these metabolites, there was only one phthalate pathway by the cultivable pyrene degrader *Sphingomonas sp.* YT1005.

In CK_MFC treatments, all ten metabolites are identified (Fig. 6 and S3, Table S3). Besides those in the phthalate pathway in CK_Sph treatment, metabolite ⓖ (m/z = 427) was protocatechuic acid, a downstream metabolite of phthalic acid by dioxygenase, dehydrogenase and decarboxylase. It suggested that phthalic acid was further metabolized by the active pyrene degrading consortium enriched by MMI and entered the tricarboxylic acid (TCA) cycle via β-ketoadipate pathway. Alternatively, metabolite ⓗ (m/z = 267) was identified as 4-phenanthrenol from phenanthrene-4-carboxylic acid. Metabolite ⓘ (m/z = 206, t_R=8.47 min) and metabolite ⓙ (m/z = 206, t_R=20.87 min) was *trans*-2'-carboxybenzalpyruvate and salicylic acid, respectively. They were two downstream metabolites of 1-hydroxy-2-naphthoic acid (metabolite ⓔ). As metabolites ⓘ and ⓙ were only detectable in CK_MFC treatment, MMI-enriched active pyrene degrading consortium exhibited a unique salicylate pathway for pyrene degradation.

In the phthalate pathway, metabolites □, □, □ and □ were detected in all treatments but only on Day 10. Metabolite □ was detected on all sampling days in all treatments, whereas metabolites □ was only detectable on Day 20. These results suggested metabolites □, □, □ and □ were gradually metabolized into downstream metabolites (□ and □), which accumulated during pyrene degradation process. In the salicylate pathway, metabolite □ was detected on days 20 and 30, also suggesting a significant accumulation of downstream metabolites.

4. Discussion

In the present study, *Sphingomonas sp.* YT1005 was identified as a cultivable pyrene degrader from soils at an abandoned steel plant site. *Sphingomonas* is a typical PAH-degrading microorganism (Zhao et al 2017). *Sphingomonas* LB126 is reported to use fluorene as the sole carbon or energy source and can co-metabolize phenanthrene, fluoranthene, anthracene and dibenzothiophene (van Herwijnen et al 2003). *Sphingomonas* sp. GY2B isolated from petroleum-contaminated soils could degrade phenanthrene through the salicylate pathway (Tao et al 2007). However, the isolated strain *Sphingomonas sp.* YT1005 in this study belongs to *Sphingomonas echinoides*, which is not previously linked with pyrene degradation, and our study brought direct evidence of their functions in metabolizing pyrene.

The dominant bacterial genera in soils (*Sphingomonas*, *Arthrobacter*, *Lysobacter*, *Rhodococcus*, *Pedobacter*, *Aeromicrobium* and *Pseudonocardia*) are abundant soil bacterial lineages (Delgado-Baquerizo et al 2018) and participate in soil carbon and nitrogen cycles (Schimel and Schaeffer 2012). After pyrene degradation, the relative abundance of *Pseudonocardia*, *Streptomyces*, *Lysobacter* and *Thermomonas* significantly increased. They are reported to be responsible for PAHs biodegradation by many previous studies. *Lysobacter* is linked to pyrene degradation (Wang et al 2018) and *Thermomonas* has the capacity of degrading anthracene (Nzila et al 2018). Our findings were consistent with these reports and indicated that predominant bacterial taxa in pyrene-contaminated soils were related to pyrene tolerance or degradation.

Both bacterial α-diversity and community composition were of no significant difference between OS_NC and MMI_NC treatments, indicating that MNP-functionalization had little impacts on soil bacterial community and did not affect pyrene biodegradation process (Wang et al 2016). During the pyrene degradation process, the active pyrene degraders utilized pyrene and lost magnetism gradually, resulting in their enrichment in the magnetic-free fractions of MFCs (Zhang et al 2015). Accordingly, the community structure of MFC_Pyr was different from MFC_NC and the enriched bacterial lineages were the potential active pyrene degraders (Fig. 2B).

The active pyrene degrading consortium isolated by MMI included *Gp16*, *Streptomyces*, *Pseudonocardia*, *Panacagrimonas*, *Methylotenera* and *Nitrospira* (Fig. 3C). Among them, the roles of *Streptomyces* and *Pseudonocardia* in PAH biodegradation have been previously reported (Chaudhary et al 2011, Chen et al 2018). *Pseudonocardia* could degrade pyrene in agricultural soils (Chen et al 2018) and *Streptomyces rochei* was capable of using anthracene, fluorene, phenanthrene and pyrene as the sole carbon source

(Chaudhary et al 2011). As for other bacterial taxa, *Gp16* is reported to tolerate toxic chemicals (De et al 2003, De and Ramaiah 2007), and *Methylotenera* is a methylamine- and methanol-utilizing bacterium with denitrification capability (Kalyuzhnaya et al 2010, Mustakhimov et al 2013). *Panacagrimonas* is newly isolated from soils (Im et al 2010) and enriched in the rhizosphere of pioneer plants in metal-contaminated soils (Navarro-Noya et al 2010). *Nitrospira* is normally viewed as key nitrifiers in soils (Li et al 2019, Wang et al 2019). However, no study has ever reported their involvement in pyrene degradation, and this work broadened our understanding on pyrene-degrading microbes, suggesting that numerous soil microbes have the capability to degrade pyrene.

The relative abundance of all pyrene dioxygenase genes was higher in OS_Pyr than OS_NC treatments, hinting the enrichment of pyrene degraders harboring dioxygenase genes with pyrene amendment. Additionally, their relative abundance was around 10–200 folds higher in MFC_Pyr than OS_Pyr, proving the successful isolation of the active pyrene degrading microbes in MFC fractions (Fig. 5A). Each pyrene dioxygenase gene exhibited a positive correlation with pyrene degradation efficiency (Table 1 and Fig. 5), suggesting their critical roles in pyrene degradation. *nidA*, *nidA3* and PAH-RHDα-GP genes are reported as biomarkers for pyrene degradation in many previous studies. As a key gene for the initial hydroxylation of PAH aromatic ring, the α subunit of *nidA*-encoding dioxygenase was cloned in *Mycobacterium* sp. strain PYR-1 (Khan et al 2001, Hall et al 2005) and proved to be critical in pyrene degradation (Guo et al 2010). The relative abundance of *nidA3* gene was linked to pyrene biodegradation efficiency by PAH-degrading communities (Chen et al 2016). PAH-RHD_{α}-GP genes in the initial step of PAH aerobic metabolism demonstrated a positive correlation with PAH biodegradation potential in soils (Cebron et al 2008, Jurelevicius et al 2012). In addition, the relative abundance of all pyrene dioxygenase genes was also positively correlated with that of the potential active pyrene degraders in MFC_Pyr treatment (0.8611, $p < 0.01$), hinting that they might harbor these pyrene dioxygenase encoding genes.

Cultivable pyrene degrader *Sphingomonas sp.* YT1005 was found to degrade pyrene following the phthalate pathway. All the metabolites in CK_Sph treatments have been reported as key metabolites in the phthalate pathway by previous studies, *e.g.*, *cis*-4,5-pyrene dihydrodiol (metabolite) (Luan et al 2006, Zhong et al 2006), dihydroxyphenanthrene (metabolite) (Zhong et al 2006), 2-hydroxy-2-H-benzo[h]chromene-2-carboxylic acid (metabolite) (Wu et al 2019, Zhou et al 2016), 2-methylnaphthalene (metabolite) (Wu et al 2019) and 1-hydroxy-2-naphthoic acid (metabolite). In contrast, metabolites of protocatechuic acid (metabolite) (Jin et al 2016a), 4-phenanthrenol (metabolite) (Wu et al 2019, Zhong et al 2006), *trans*-2'-carboxybenzalpyruvate (metabolite) and salicylic acid (metabolite) (Zhou et al 2016, Zhong et al 2017) are involved in the salicylate pathway of PAHs degradation. Thus, MMI-isolated pyrene degrading consortium metabolized pyrene through both phthalate and salicylate pathways (Fig. 6). Both phthalate and salicylate pathways are important in pyrene metabolism (Sun et al 2019) and previously reported for the degradation of other PAHs. Pyrene-degrading strains mainly exhibit the phthalate pathway for pyrene (Liang et al 2006, Jin et al 2016b). Only few studies suggested the involvement of salicylate pathway in pyrene degradation, such as *Mycobacterium sp.* WY10 which degrades pyrene predominantly in the phthalate pathway and minorly in the salicylate pathway (Sun et al

2019). The extra salicylate pathway imposed by MMI-isolated pyrene degrading consortium suggested a more complex pyrene degradation pathways in natural habitats than individual pyrene-degrading strains (Zafra et al 2017, Gallego et al 2014), hinting a underestimated diversity of pyrene degraders. MMI is therefore an effective approach to separate the active pyrene degraders from soil matrices, not only helping in building up high-efficient degrading consortiums for bioaugmentation but also contributing to our deeper understanding on the actual players and pathways for pyrene metabolism in soils.

Enhanced pyrene degradation performance by bioaugmentation with soil indigenous microbes has been reported in many previous studies (Chen et al 2016, Wang et al 2018). However, bioaugmentation postpone or even failure commonly occurs, generally explained by microbial acclimation to environment changes, *e.g.*, morphological, physiological and behavioral adjustments (Ren et al 2018, Macleod and Semple 2006). In the present study, bioaugmentation with *Sphingomonas sp.* YT1005 in either sterile soils (CK_Sph) or original soils (BA_Sph) did not have satisfactory pyrene degradation performance (Fig. 1), attributing to the complex bacterial intra-correlations within the bacterial community. Pyrene degradation efficiency was consistent between OS_Pyr and CK_MFC treatments, proving that MMI-enriched bacterial consortium had the same pyrene degradation capability comparing to indigenous microbiota. Accordingly, the enriched bacterial consortium consisting of *Gp16*, *Streptomyces*, *Pseudonocardia*, *Panacagrimonas*, *Methylotenera* and *Nitrospira* was responsible for *in-situ* pyrene degradation. However, *Sphingomonas sp.* exhibited negative correlations with those active pyrene degraders (Fig. 4), and the introduction of *Sphingomonas sp.* in BA_Sph treatments therefore inhibited their activities and consequently resulted in bioaugmentation postpone. This explanation was consistent with some previous studies that the correlation between pure-cultivation isolated and indigenous degraders affected the bioaugmentation performance. Non-active degrader *Marmoricola* LJ-33 significantly enhanced biphenyl degradation efficiency in soils by changing bacterial diversity in biphenyl metabolism (Li et al 2020). Another bioaugmentation by PAH-degrader *Acinetobacter tandoii* LJ-5 produced a significant increased phenanthrene mineralization, attributing to the altered diversity of the active phenanthrene degraders, instead of *Acinetobacter tandoii* LJ-5 itself (Li et al 2018). We then propose the mechanism explaining bioaugmentation performance regarding intra-correlations between cultivable and active pyrene degraders (Fig. 7). Ehanced bioaugmentation is expected when these two groups of bacteria exhibit positive intra-correlations, whereas negative intra-correlations between cultivable and active pyrene degraders consequently result in bioagumentation postpone or failure. As for neutral intra-correlations, the effectiveness and performance of bioaugmentation is non-deterministic and potentially dependent on other environmental variables.

5. Conclusion

This study investigated soil pyrene degraders via both cultivation-dependent and cultivation-dependent approaches. *Sphingomonas sp.* YT1005 was isolated via pure cultivation, and the active pyrene degrading consortium consisting of *Gp16*, *Streptomyces*, *Pseudonocardia*, *Panacagrimonas*, *Methylotenera* and *Nitrospira* was isolated by MMI. An unexpected postpone of pyrene degradation was found in bioaugmentation with *Sphingomonas sp.* YT1005, explained by its negative intra-correlations

with the active pyrene degraders. In contrast, bioaugmentation with MMI-isolated pyrene degrading consortium significantly accelerated pyrene degradation in soils. It was supported by the increasing relative abundance of pyrene dioxygenase encoding genes (*nidA*, *nidA3* and PAH-RHDα-GP) along with pyrene degradation efficiency. Further analysis of pyrene degradation pathway suggested that *Sphingomonas sp.* YT1005 only exhibited the phthalate pathway, whereas MMI-isolated pyrene degraders possessed both phthalate and salicylate pathways. This work broadens our vision on the actual pyrene degradation process and mechanisms in soils, suggesting that intra-correlations between the introduced degraders and the indigenous active degraders are key factors determining bioaugmentation performance. Isolating and reintroducing the active indigenous active degraders is a more promising strategy for bioaugmentation.

Declarations

Acknowledgments

Financial support was provided by the National Natural Science Foundation of China (41807119), the Natural Science Foundation of Beijing, China (8212030), Special Fund of State Key Joint Laboratory of Environment Simulation and Pollution Control (19K04ESPCT), Fundamental Research Funds for the Central Universities (FRF-TP-20-010A3), the Open Fund of National Engineering Laboratory for Site Remediation Technologies (NEL-SRT201907), and Beijing Municipal Science and Technology Project (Z181100002418016). DZ also acknowledges the support of Chinese Government's Thousand Talents Plan for Young Professionals.

Author Contribution Statement

BJ and DZ contributed to the conception and design of the study. YC, NZ, LL and YS did the lab work. YC and BJ did the data analysis. GS and ZL collected the soil samples and performed the statistical analysis. YC and BJ drafted the manuscript. XW, HZ, YX and DZ revised the manuscript. All authors approved the submitted version.

Ethics declarations

Ethics approval and consent to participate

Not applicable

Consent for publication

Not applicable

Competing interests

The authors declare no competing interests.

References

1. Ghosal D, Ghosh S, Dutta TK, Ahn Y. Current state of knowledge in microbial degradation of Polycyclic Aromatic Hydrocarbons (PAHs): A review. Front Microbiol. 2016;7:1369.
2. Kanaly RA, Harayama S. Biodegradation of high-molecular-weight polycyclic aromatic hydrocarbons by bacteria. J Bacteriol. 2000;182:2059–67.
3. Duan L, Naidu R, Thavamani P, Meaklim J, Megharaj M. Managing long-term polycyclic aromatic hydrocarbon contaminated soils: a risk-based approach. Environ Sci Pollut R. 2015;22:8927–41.
4. Wang C, Wu S, Zhou S, Sill Y, Song J. Characteristics and Source Identification of Polycyclic Aromatic Hydrocarbons (PAHs) in Urban Soils: A Review. Pedosphere. 2017a;27:17–26.
5. Nam JJ, Thomas GO, Jaward FM, Steinnes E, Gustafsson O. Jones KC PAHs in background soils from Western Europe: Influence of atmospheric deposition and soil organic matter. Chemosphere. 2008;70:1596–602.
6. Liu Y, Gao P, Su J, da Silva EB, de Oliveira LM, Townsend T, et al. PAHs in urban soils of two Florida cities: Background concentrations, distribution, and sources. Chemosphere. 2019;214:220–7.
7. Okere UV, Schuster JK, Ogbonnaya UO, Jones KC, Semple KT, Indigenous. C-14-phenanthrene biodegradation in "pristine" woodland and grassland soils from Norway and the United Kingdom. Environ Sci-Proc Imp. 2017;19:1437–44.
8. Wang J, Zhang X, Ling W, Liu R, Liu J, Kang F, et al. Contamination and health risk assessment of PAHs in soils and crops in industrial areas of the Yangtze River Delta region, China. Chemosphere. 2017b;168:976–87.
9. Kim K-H, Jahan SA, Kabir E. Brown RJC A review of airborne polycyclic aromatic hydrocarbons (PAHs) and their human health effects. Environ Int. 2013;60:71–80.
10. Peng R, Xiong A, Xue Y, Fu X, Gao F, Zhao W, et al. Microbial biodegradation of polyaromatic hydrocarbons. FEMS MicroBiol Rev. 2008;32:927–55.
11. Haleyur N, Shahsavari E, Taha M, Khudur LS, Koshlaf E, Osborn AM, et al. Assessing the degradation efficacy of native PAH-degrading bacteria from aged, weathered soils in an Australian former gasworks site. Geoderma. 2018;321:110–7.
12. Zeng J, Zhu Q, Wu Y, Chen H, Lin X. Characterization of a polycyclic aromatic ring-hydroxylation dioxygenase from Mycobacterium sp NJS-P. Chemosphere. 2017;185:67–74.
13. Segura A, Hernandez-Sanchez V, Marques S, Molina L. Insights in the regulation of the degradation of PAHs in Novosphingobium sp HR1a and utilization of this regulatory system as a tool for the detection of PAHs. Sci Total Environ. 2017;590:381–93.
14. Cebron A, Norini M-P, Beguiristain T, Leyval C, Real-Time. PCR quantification of PAH-ring hydroxylating dioxygenase (PAH-RHD alpha) genes from Gram positive and Gram negative bacteria in soil and sediment samples. J Microbiol Methods. 2008;73:148–59.
15. Pinyakong O, Habe H, Yoshida T, Nojiri H, Omori T. Identification of three novel salicylate 1-hydroxylases involved in the phenanthrene degradation of *Sphingobium* sp strain P2. Biochem

Biophys Res Commun. 2003;301:350–7.

16. Denome SA, Stanley DC, Olson ES, Young KD. Metabolism of dibenzothiophene and naphthalene in Pseudomonas strains: complete DNA sequence of an upper naphthalene catabolic pathway. Journal Of Bacteriology. 1993;175:6890–901.
17. Schuler L, Chadhain SMN, Jouanneau Y, Meyer C, Zylstra GJ, Hols P, et al. Characterization of a novel angular dioxygenase from fluorene-degrading Spingomonas sp strain LB126. Appl Environ Microbiol. 2008;74:1050–7.
18. Izmalkova TY, Sazonova OI, Kosheleva IA, Boronin AM. Phylogenetic Analysis of the Genes for Naphthalene and Phenanthrene Degradation in Burkholderia sp Strains. Russ J Genet. 2013;49:609–16.
19. Bosch R, Garcia-Valdes E, Moore ERB. Complete nucleotide sequence and evolutionary significance of a chromosomally encoded naphthalene-degradation lower pathway from Pseudomonas stutzeri AN10. Gene. 2000;245:65–74.
20. Liu T, Xu Y, Liu H, Luo S, Yin Y, Liu S, et al. Functional characterization of a gene cluster involved in gentisate catabolism in *Rhodococcus* sp. strain NCIMB 12038. Appl Microbiol Biotechnol. 2011;90:671–8.
21. Stingley RL, Khan AA, Cerniglia CE. Molecular characterization of a phenanthrene degradation pathway in Mycobacterium vanbaalenii PYR-1. Biochem Biophys Res Commun. 2004;322:133–46.
22. Chen S, Peng J, Duan G. Enrichment of functional microbes and genes during pyrene degradation in two different soils. J Soil Sediment. 2016;16:417–26.
23. Takizawa N, Iida T, Sawada T, Yamauchi K, Wang YW, Fukuda M, et al. Nucleotide sequences and characterization of genes encoding naphthalene upper pathway of pseudomonas aeruginosa PaK1 and Pseudomonas putida OUS82. J Biosci Bioeng. 1999;87:721–31.
24. Krivobok S, Kuony S, Meyer C, Louwagie M, Willison JC, Jouanneau Y. Identification of pyrene-induced proteins in Mycobacterium sp strain 6PY1: Evidence for two ring-hydroxylating dioxygenases. Journal Of Bacteriology. 2003;185:3828–41.
25. Saito A, Iwabuchi T, Harayama S. Characterization of genes for enzymes involved in the phenanthrene degradation in Nocardioides sp. KP7. Chemosphere. 1999;38:1331–7.
26. Johnsen AR, Wick LY, Harms H. Principles of microbial PAH-degradation in soil. Environ Pollut. 2005;133:71–84.
27. Nzila A. Update on the cometabolism of organic pollutants by bacteria. Environ Pollut. 2013;178:474–82.
28. Jiang Y, Zhang Z, Zhang X. Co-biodegradation of pyrene and other PAHs by the bacterium Acinetobacter johnsonii. Ecotox Environ Safe. 2018a;163:465–70.
29. Vaidya S, Jain K, Madamwar D. Metabolism of pyrene through phthalic acid pathway by enriched bacterial consortium composed of *Pseudomonas*, *Burkholderia*, and *Rhodococcus* (PBR). 3 Biotech. 2017;7:29.

30. Rabodonirina S, Rasolomampianina R, Krier F, Drider D, Merhaby D, Net S, et al. Degradation of fluorene and phenanthrene in PAHs-contaminated soil using Pseudomonas and Bacillus strains isolated from oil spill sites. J Environ Manage. 2018;232:1–7.
31. Wu F, Guo C, Liu S, Liang X, Lu G, Dang Z. Pyrene Degradation by Mycobacterium gilvum: Metabolites and Proteins Involved. *Water Air Soil Poll*. 2019;230.
32. Khan S, Gupta S, Gupta N. Dearomatization of diesel oil using Pseudomonas sp. Biotechnol Lett. 2018;40:1329–33.
33. Jia X, He Y, Huang L, Jiang D, Lu W. n-Hexadecane and pyrene biodegradation and metabolization by Rhodococcus sp. T1 isolated from oil contaminated soil. Chin J Chem Eng. 2019;27:411–7.
34. Guo G, Tian F, Ding K, Wang L, Liu T, Yang F. Bacterial Communities Predominant in the Degradation of C-13-Labeled Pyrene in Red Soil. Soil Sediment Contamination. 2017;26:709–21.
35. Zhou H, Guo C, Wong YS, Tam N. Genetic diversity of dioxygenase genes in polycyclic aromatic hydrocarbon-degrading bacteria isolated from mangrove sediments. FEMS Microbiol Lett. 2006;262:148–57.
36. Perelo LW. Review: In situ and bioremediation of organic pollutants in aquatic sediments. J Hazard Mater. 2010;177:81–9.
37. Li J, Luo C, Zhang D, Song M, Cai X, Jiang L, et al. Autochthonous Bioaugmentation-Modified Bacterial Diversity of Phenanthrene Degraders in PAH-Contaminated Wastewater as Revealed by DNA-Stable Isotope Probing. Environ Sci Technol. 2018;52:2934–44.
38. Mohanrasu K, Premnath N, Prakash GS, Sudhakar M, Boobalan T, Arun A. Exploring multi potential uses of marine bacteria; an integrated approach for PHB production, PAHs and polyethylene biodegradation. J Photochem Photobiol B-Biol. 2018;185:55–65.
39. Major DW, McMaster ML, Cox EE, Edwards EA, Dworatzek SM, Hendrickson ER, et al. Field demonstration of successful bioaugmentation to achieve dechlorination of tetrachloroethene to ethene. Environ Sci Technol. 2002;36:5106–16.
40. Wu H, Shen J, Jiang X, Liu X, Sun X, Li J, et al. Bioaugmentation strategy for the treatment of fungicide wastewater by two triazole-degrading strains. Chem Eng J. 2018;349:17–24.
41. Dybas MJ, Hyndman DW, Heine R, Tiedje J, Linning K, Wiggert D, et al. Development, operation, and long-term performance of a full-scale biocurtain utilizing bioaugmentation. Environ Sci Technol. 2002;36:3635–44.
42. Heinaru E, Merimaa M, Viggor S, Lehiste M, Leito I, Truu J, et al. Biodegradation efficiency of functionally important populations selected for bioaugmentation in phenol- and oil-polluted area. FEMS Microbiol Ecol. 2005;51:363–73.
43. Sørensen SJ, Tim S, Regin R. Predation by protozoa on *Escherichia coli* K12 in soil and transfer of resistance plasmid RP4 to indigenous bacteria in soil. Appl Soil Ecol. 1999;11:79–90.
44. Mrozik A, Piotrowska-Seget Z. Bioaugmentation as a strategy for cleaning up of soils contaminated with aromatic compounds. Microbiological research. 2010;165:363–75.

45. Thompson IP, van der Gast CJ, Ciric L. Singer AC Bioaugmentation for bioremediation: the challenge of strain selection. Environ Microbiol. 2005;7:909–15.
46. Kaeberlein T, Lewis K, Epstein SS. Isolating "uncultivable" microorganisms in pure culture in a simulated natural environment. Science. 2002;296:1127–9.
47. Vartoukian SR, Palmer RM. Wade WG Strategies for culture of 'unculturable' bacteria. FEMS Microbiol Lett. 2010;309:1–7.
48. Jiang B, Jin N, Xing Y, Su Y, Zhang D Unraveling uncultivable pesticide degraders via stable isotope probing (SIP). *Critical reviews in biotechnology*. 2018b;38:1025–1048.
49. Zhang D, Berry JP, Zhu D, Wang Y, Chen Y, Jiang B, et al. Magnetic nanoparticle-mediated isolation of functional bacteria in a complex microbial community. Isme Journal. 2015;9:603–14.
50. Zhao X, Li H, Ding A, Zhou G, Sun Y, Zhang D. Preparing and characterizing Fe3O4@cellulose nanocomposites for effective isolation of cellulose-decomposing microorganisms. Mater Lett. 2016;163:154–7.
51. Sun Y, Yin M, Zheng D, Wang T, Zhao X, Luo C, et al. Different acetonitrile degraders and degrading genes between anaerobic ammoniumoxidation and sequencing batch reactor as revealed by stable isotope probing and magnetic-nanoparticle mediated isolation. Sci Total Environ. 2021;758:143588.
52. Zhang D, Fakhrullin RF, Özmen M, Wang H, Wang J, Paunov VN, et al. Functionalization of whole-cell bacterial reporters with magnetic nanoparticles. Microb Biotechnol. 2011;4:89–97.
53. Wang X, Zhao X, Li H, Jia J, Liu Y, Ejenavi O, et al. Separating and characterizing functional alkane degraders from crude-oil-contaminated sites via magnetic nanoparticle-mediated isolation. Res Microbiol. 2016;167:731–44.
54. Zhang D, He Y, Wang Y, Wang H, Wu L, Aries E, et al. Whole-cell bacterial bioreporter for actively searching and sensing of alkanes and oil spills. Microbial biotechnology. 2012;5:87–97.
55. Guo C, Dang Z, Wong Y, Tam NF. Biodegradation ability and dioxgenase genes of PAH-degrading Sphingomonas and Mycobacterium strains isolated from mangrove sediments. Int Biodeterior Biodegradation. 2010;64:419–26.
56. Song M, Luo C, Jiang L, Zhang D, Wang Y, Zhang G, et al. Identification of Benzo[a]pyrene-Metabolizing Bacteria in Forest Soils by Using DNA-Based Stable-Isotope Probing. Appl Environ Microbiol. 2015;81:7368–76.
57. Hamady M, Lozupone C, Knight R. Fast UniFrac: facilitating high-throughput phylogenetic analyses of microbial communities including analysis of pyrosequencing and PhyloChip data. The ISME Journal. 2010;4:17–27.
58. Deng S, Ke T, Li L, Cai S, Zhou Y, Liu Y, et al. Impacts of environmental factors on the whole microbial communities in the rhizosphere of a metal-tolerant plant: *Elsholtzia haichowensis* Sun. Environ Pollut. 2018;237:1088–97.
59. Zhao H, Zhang Y, Xiao X, Li G, Zhao Y, Liang Y. Different phenanthrene-degrading bacteria cultured by in situ soil substrate membrane system and traditional cultivation. Int Biodeterior Biodegradation. 2017;117:269–77.

60. van Herwijnen R, Wattiau P, Bastiaens L, Daal L, Jonker L, Springael D, et al. Elucidation of the metabolic pathway of fluorene and cometabolic pathways of phenanthrene, fluoranthene, anthracene and dibenzothiophene by Sphingomonas sp LB126. Res Microbiol. 2003;154:199–206.
61. Tao X, Lu G, Dang Z, Yang C. Yi X A phenanthrene-degrading strain *Sphingomonas* sp GY2B isolated from contaminated soils. Process biochemistry. 2007;42:401–8.
62. Delgado-Baquerizo M, Oliverio AM, Brewer TE, Benavent-Gonzalez A, Eldridge DJ, Bardgett RD, et al. A global atlas of the dominant bacteria found in soil. Science. 2018;359:320–5.
63. Schimel JP, Schaeffer SM. Microbial control over carbon cycling in soil. Front Microbiol. 2012;3:348.
64. Wang B, Teng Y, Xu Y, Chen W, Ren W, Li Y, et al. Effect of mixed soil microbiomes on pyrene removal and the response of the soil microorganisms. Sci Total Environ. 2018;640:9–17.
65. Nzila A, Sankara S, Al-Momani M, Musa MM. Isolation and characterisation of bacteria degrading polycyclic aromatic hydrocarbons: phenanthrene and anthracene. Archives of Environmental Protection. 2018;44:43–54.
66. Chaudhary P, Sharma R, Singh SB, Nain L. Bioremediation of PAH by *Streptomyces* sp. Bull Environ Contam Toxicol. 2011;86:268–71.
67. Chen S, Duan G, Ding K, Huang F, Zhu. Y DNA stable-isotope probing identifies uncultivated members of *Pseudonocardia* associated with biodegradation of pyrene in agricultural soil. FEMS Microbiol Ecol. 2018;94:fiy026.
68. De J, Ramaiah N, Mesquita A, Verlekar X. Tolerance to various toxicants by marine bacteria highly resistant to mercury. Mar Biotechnol. 2003;5:185–93.
69. De J, Ramaiah N. Characterization of marine bacteria highly resistant to mercury exhibiting multiple resistances to toxic chemicals. Ecol Ind. 2007;7:511–20.
70. Kalyuzhnaya MG, Beck DAC, Suciu D, Pozhitkov A, Lidstrom ME. Chistoserdova L Functioning in situ: gene expression in Methylotenera mobilis in its native environment as assessed through transcriptomics. ISME J. 2010;4:388–98.
71. Mustakhimov I, Kalyuzhnaya MG, Lidstrom ME, Chistoserdova L. Insights into Denitrification in Methylotenera mobilis from Denitrification Pathway and Methanol Metabolism Mutants. Journal Of Bacteriology. 2013;195:2207–11.
72. Im WT, Liu QM, Yang JE, Kim MS, Kim SY, Lee ST, et al. Panacagrimonas perspica gen. nov., sp nov., a novel member of Gammaproteobacteria isolated from soil of a ginseng field. Journal Of Microbiology. 2010;48:262–6.
73. Navarro-Noya YE, Jan-Roblero J, del Carmen González-Chávez M, Hernández-Gama R. Hernández-Rodríguez C Bacterial communities associated with the rhizosphere of pioneer plants (Bahia xylopoda and Viguiera linearis) growing on heavy metals-contaminated soils. Antonie Van Leeuwenhoek. 2010;97:335–49.
74. Li C, Hu H, Chen Q, Chen D, He J. *Comammox Nitrospira* play an active role in nitrification of agricultural soils amended with nitrogen fertilizers. Soil Biol Biochem. 2019;138:107609.

75. Wang Z, Cao Y, Zhu-Barker X, Nicol GW, Wright AL, Jia Z, et al. *Comammox Nitrospira* clade B contributes to nitrification in soil. Soil Biol Biochem. 2019;135:392–5.
76. Khan AA, Wang R, Cao W, Doerge DR, Wennerstrom D, Cerniglia CE. Molecular cloning, nucleotide sequence, and expression of genes encoding a polcyclic aromatic ring dioxygenase from *Mycobacterium* sp strain PYR-1. Appl Environ Microbiol. 2001;67:3577–85.
77. Hall K, Miller C, Sorensen DL, Anderson AJ, Sims RC. Development of a catabolically significant genetic probe for polycyclic aromatic hydrocarbon-degrading Mycobacteria in soil. Biodegradation. 2005;16:475–84.
78. Jurelevicius D, Alvarez VM, Peixoto R, Rosado AS, Seldin L. Bacterial polycyclic aromatic hydrocarbon ring-hydroxylating dioxygenases (PAH-RHD) encoding genes in different soils from King George Bay, Antarctic Peninsula. Appl Soil Ecol. 2012;55:1–9.
79. Luan T, Yu KSH, Zhong Y, Zhou H, Lan C. Tam NFY Study of metabolites from the degradation of polycyclic aromatic hydrocarbons (PAHs) by bacterial consortium enriched from mangrove sediments. Chemosphere. 2006;65:2289–96.
80. Zhong Y, Luan T, Zhou H, Lan C, Tam N. Metabolite production in degradation of pyrene alone or in a mixture with another polycyclic aromatic hydrocarbon by *Mycobacterium* sp. Environ Toxicol Chem. 2006;25:2853–9.
81. Zhou H, Wang H, Huang Y, Fang T. Characterization of pyrene degradation by halophilic Thalassospira sp strain TSL5-1 isolated from the coastal soil of Yellow Sea, China. Int Biodeterior Biodegradation. 2016;107:62–9.
82. Jin J, Yao J, Zhang Q. Biodegradation of Phenanthrene by Pseudomonas sp JPN2 and Structure-Based Degrading Mechanism Study. Bull Environ Contam Toxicol. 2016a;97:689–94.
83. Zhong J, Luo L, Chen B, Sha S, Qing Q, Tam N, et al. Degradation pathways of 1-methylphenanthrene in bacterial *Sphingobium* sp MP9-4 isolated from petroleum-contaminated soil. Mar Pollut Bull. 2017;114:926–33.
84. Sun S, Wang H, Chen Y, Lou J, Wu L, Xu J. Salicylate and phthalate pathways contributed differently on phenanthrene and pyrene degradations in Mycobacterium sp. WY10. J Hazard Mater. 2019;364:509–18.
85. Liang Y, Gardner DR, Miller CD, Chen D, Anderson AJ, Weimer BC, et al. Study of biochemical pathways and enzymes involved in pyrene degradation by Mycobacterium sp strain KMS. Appl Environ Microbiol. 2006;72:7821–8.
86. Jin J, Yao J, Zhang Q, Liu J. Biodegradation of pyrene by pseudomonas sp JPN2 and its initial degrading mechanism study by combining the catabolic nahAc gene and structure-based analyses. Chemosphere. 2016b;164:379–86.
87. Zafra G, Absalón ÁE, Anducho-Reyes M, Fernandez FJ. Cortés-Espinosa DV Construction of PAH-degrading mixed microbial consortia by induced selection in soil. Chemosphere. 2017;172:120–6.
88. Gallego S, Vila J, Tauler M, Nieto JM, Breugelmans P, Springael D, et al. Community structure and PAH ring-hydroxylating dioxygenase genes of a marine pyrene-degrading microbial consortium.

Biodegradation. 2014;25:543–56.

89. Ren X, Zeng G, Tang L, Wang J, Wan J, Liu Y, et al. Sorption, transport and biodegradation - An insight into bioavailability of persistent organic pollutants in soil. Sci Total Environ. 2018;610:1154–63.
90. Macleod CJA, Semple KT. The influence of single and multiple applications of pyrene on the evolution of pyrene catabolism in soil. Environ Pollut. 2006;139:455–60.
91. Li J, Peng K, Zhang D, Luo C, Cai X, Wang Y, et al. Autochthonous bioaugmentation with non-direct degraders: A new strategy to enhance wastewater bioremediation performance. Environ Int. 2020;136:105473.

Figures

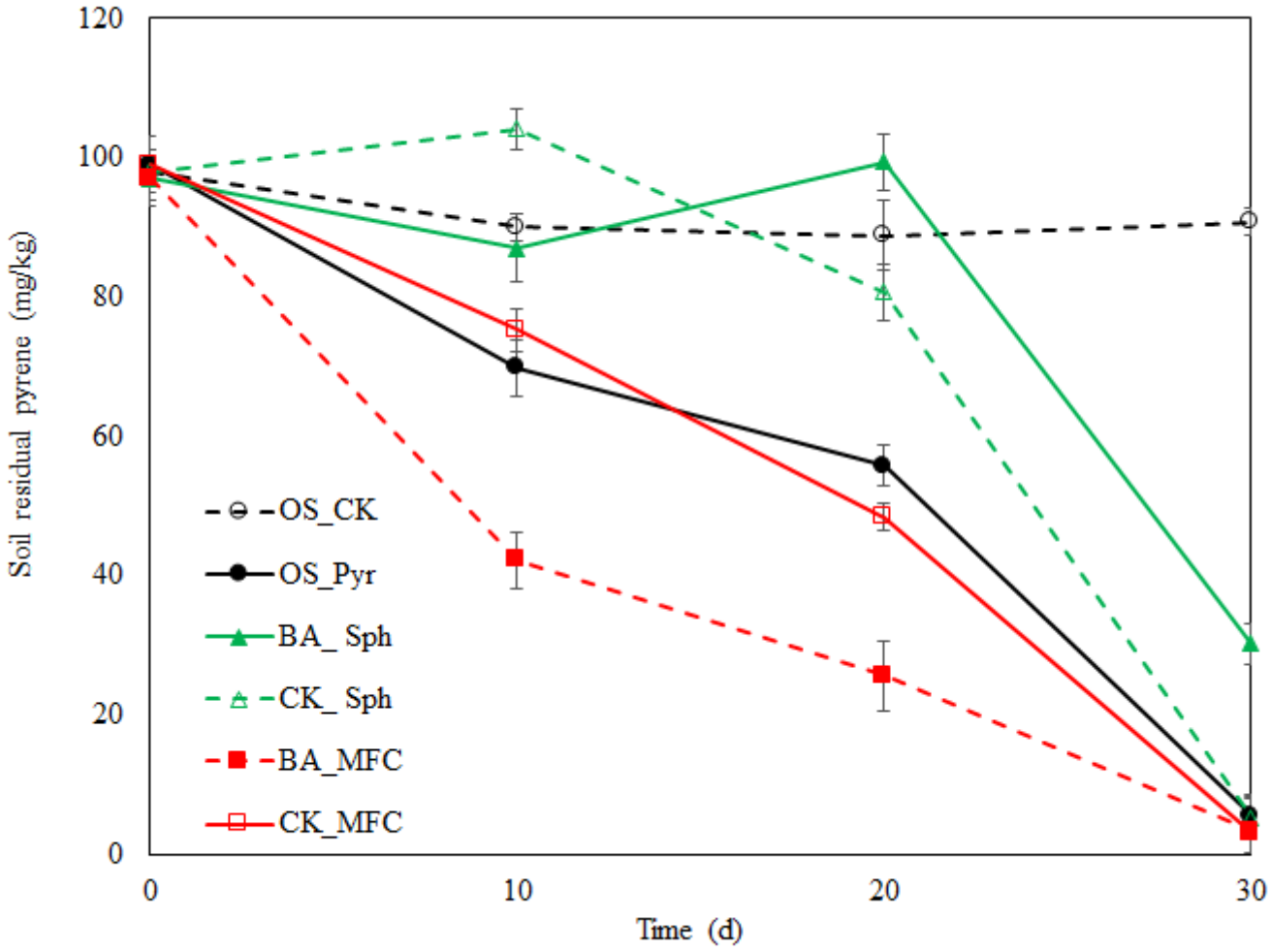

Figure 1

Pyrene degradation curves in different treatments. OS_CK represents the sterile soils with pyrene amendment. OS_Pyr represents the original soil treatments with pyrene amendment. BA_Sph refers to bioaugmentation treatment with original soils, pyrene and Sphingomonas sp. YT1005. CK_Sph refers to

bioaugmentation treatment with sterile soils, pyrene and Sphingomonas sp. YT1005. BA_MFC refers to bioaugmentation treatment with original soils, pyrene and MMI-enriched pyrene degrading consortium.CK_MFC refers to bioaugmentation treatment with sterile soils, pyrene and MMI-enriched pyrene degrading consortium.

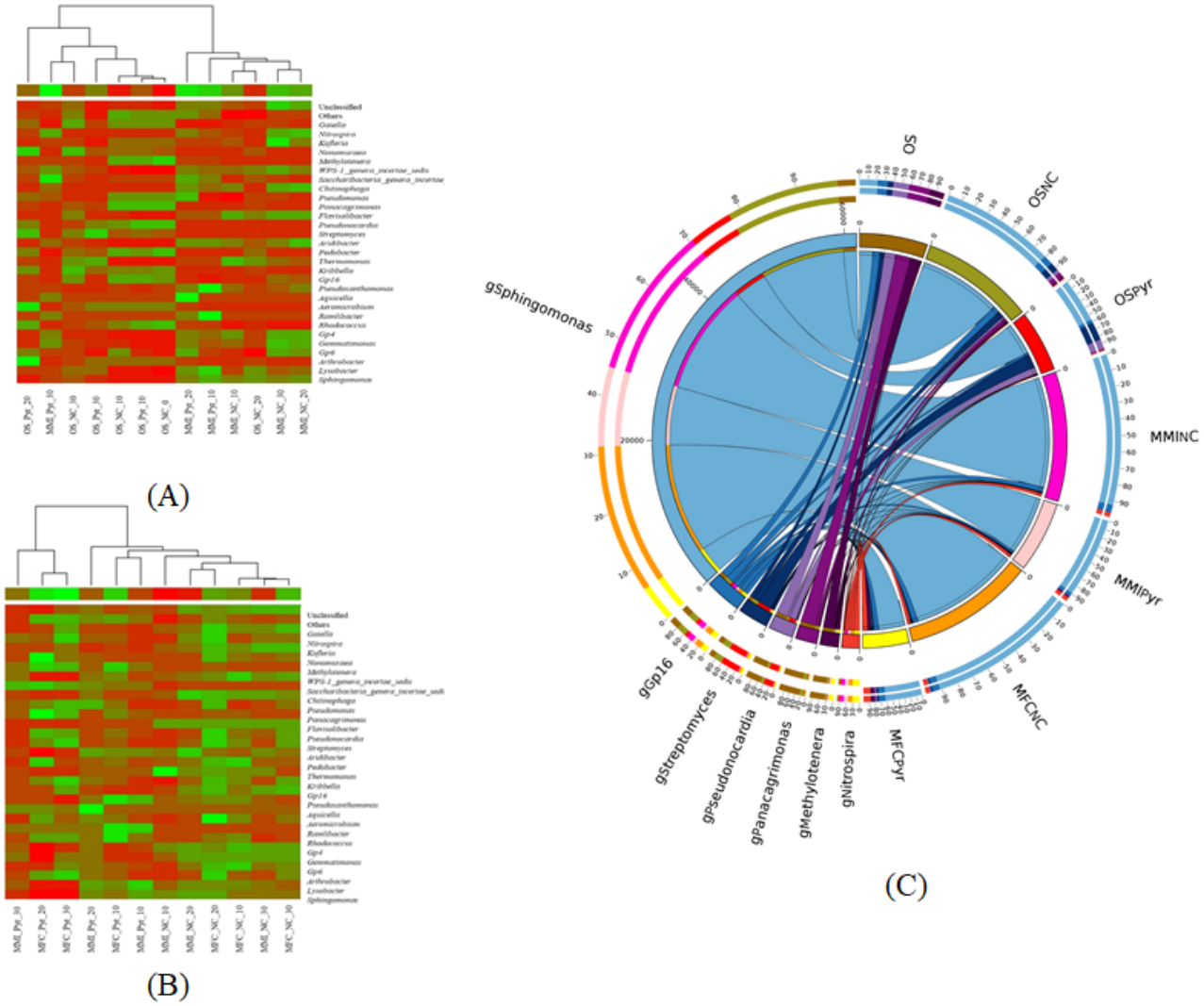

Figure 2

(A) Bray-Curtis metric distance of bacterial community compositions between OS_NC, OS_Pyr, MMI_NC and MMI_Pyr treatments on genus level. (B) Bray-Curtis metric distance of bacterial community compositions between MMI_NC, MMI_Pyr, MFC_NC and MFC_Pyr treatments on genus level. Color blocks represent the relative abundance of each bacterial general, wherein the redder color indicates the higher relative abundance. '_10', '_20' and '_30' represented samples collected on 10, 20 and 30 days, respectively.

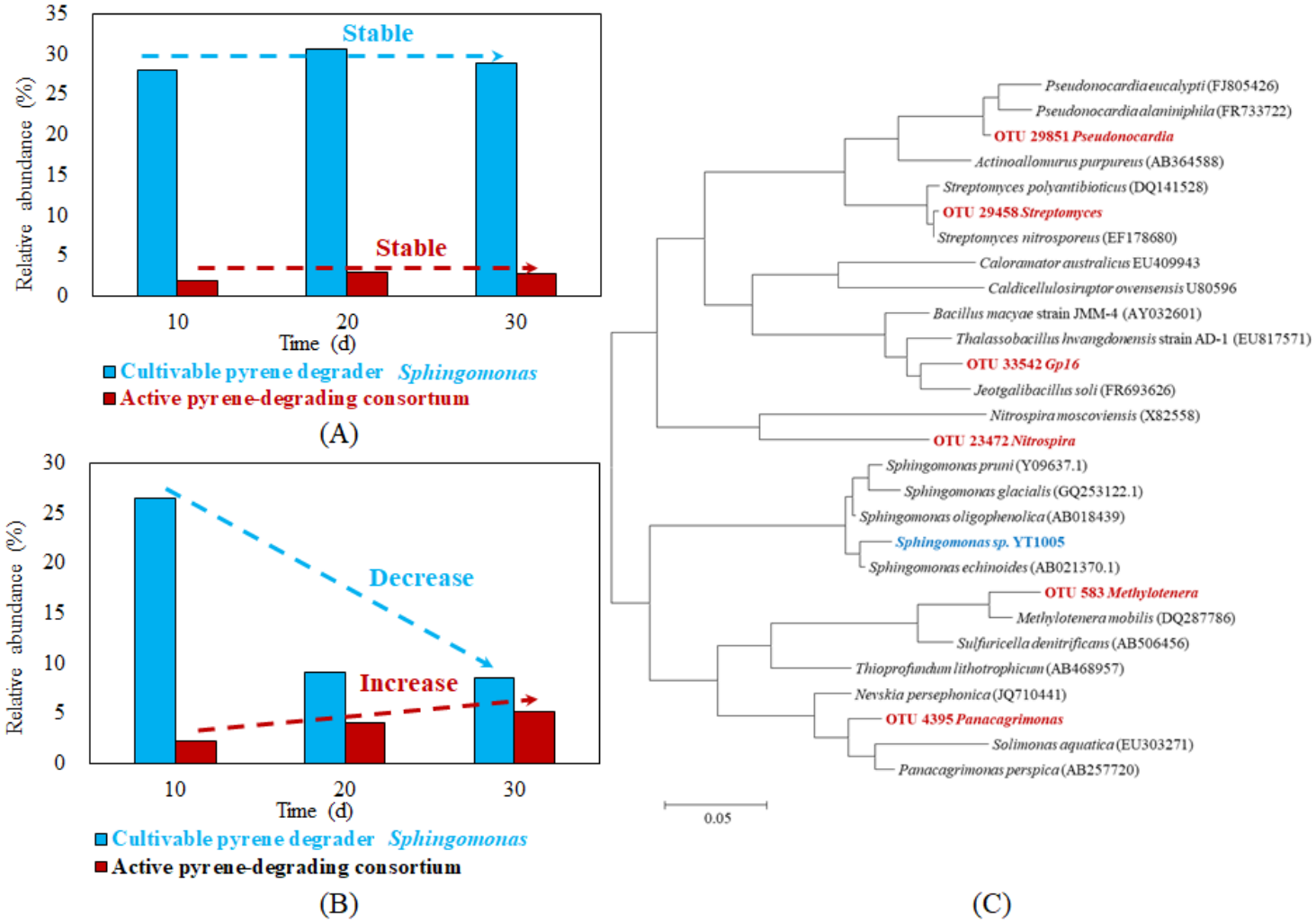

Figure 3

(A) The relative abundance of Sphingomonas sp. YT1005 and the active pyrene degraders in MFC_NC (no pyrene) throughout the incubation process. (B) The relative abundance of Sphingomonas sp. YT1005 and the active pyrene degraders in MFC_Pyr (amendment with pyrene) throughout the incubation process. (C) The phylogenetic tree of cultivable pyrene degrader Sphingomonas sp. YT1005 (OTU33525) and the potential active pyrene degraders, including Nitrospira (OTU23472), Gp16 (OTU33542), Streptomyces (OTU29458), Pseudonocardia (OTU29851), Panacagrimonas (OTU4395) and Methylotenera (OTU583).

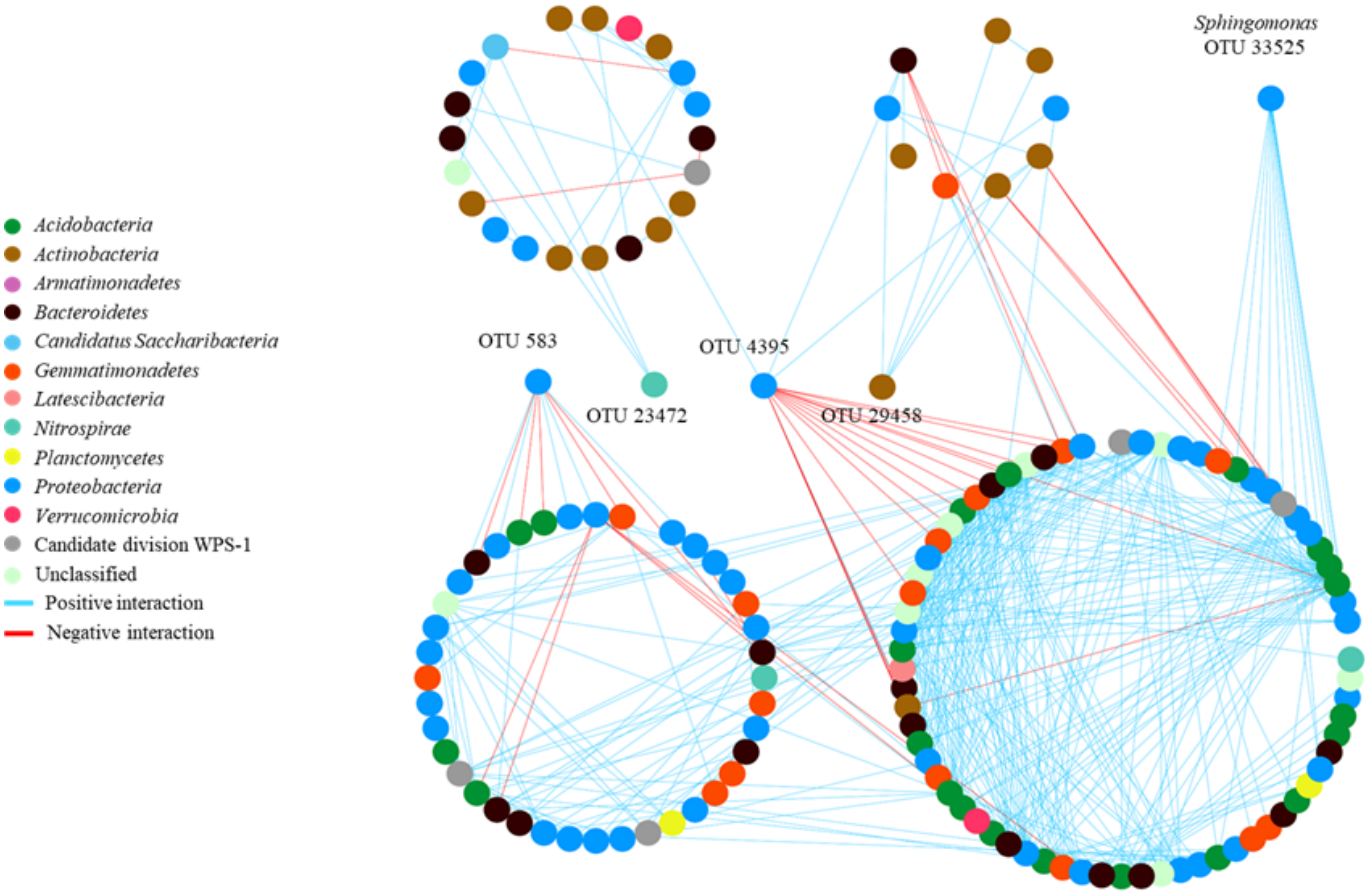

Figure 4

The co-occurrence molecular ecological network constructed based on core OTUs with the abundance > 0.5% and occurrence in over 10 of all 19 samples. Blue and red edges represent positive or negative correlations, respectively. Each point (node) stands for one OTU and the edges represent the correlations between connected OTUs. Only the modules with member number > 5 and correlated with cultivable or active pyrene-degraders were kept. OTU33525 represents the cultivable pyrene degrader Sphingomonas sp. YT1005. Core OTUs representing the active pyrene degraders include Nitrospira (OTU23472), Streptomyces (OTU29458), Panacagrimonas (OTU4395) and Methylotenera (OTU583). The other two active pyrene degraders, Gp16 (OTU33542) and Pseudonocardia (OTU29851), are not core OTUs in the molecular ecological network and not illustrated.

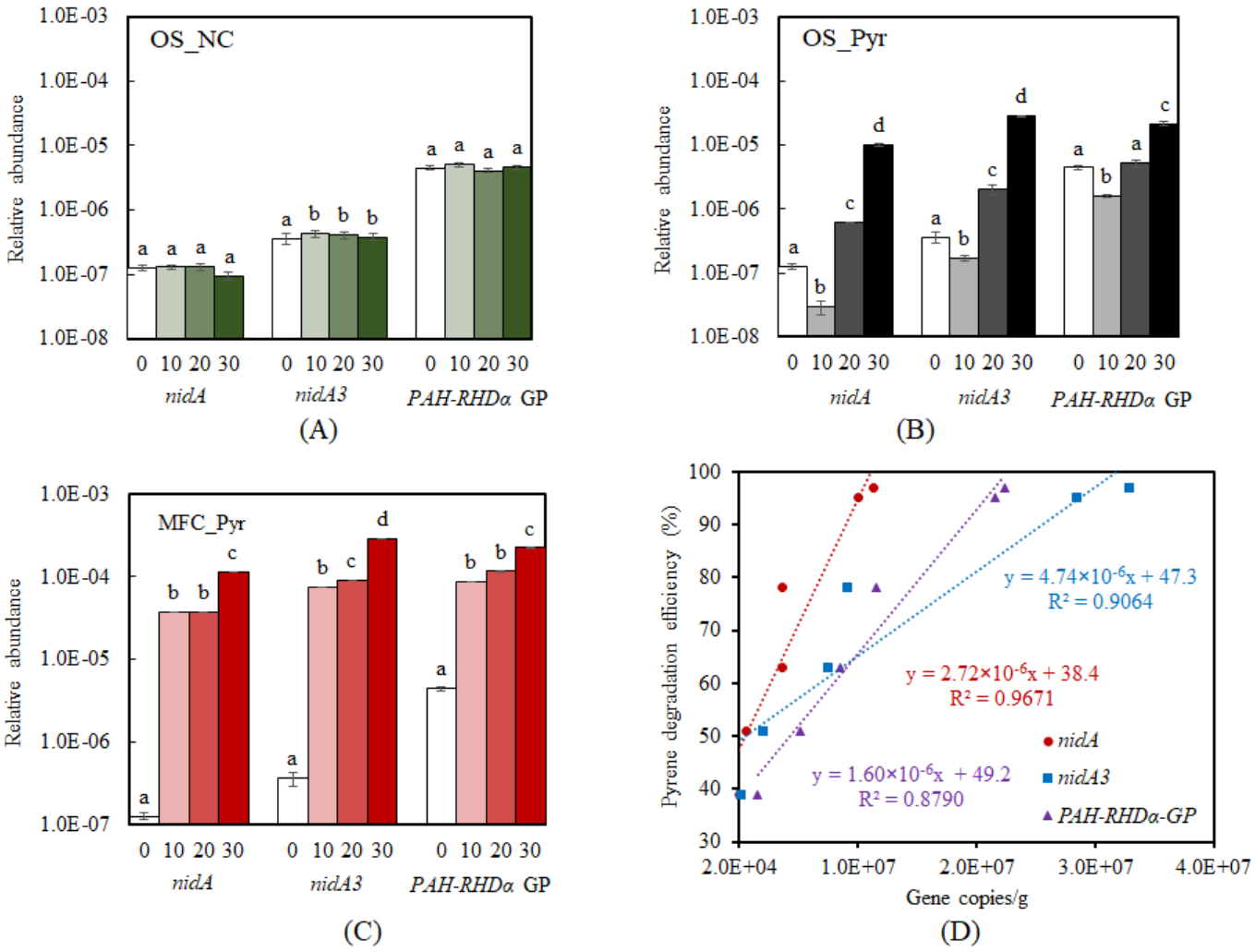

Figure 5

The relative abundance of pyrene dioxygenase encoding genes (nidA, nidA3 and PAH-RHDα-GP) in OS_NC (A), OS_Pyr (B) and MMI_Pyr (C) treatments during 30-day pyrene degradation process. (D) Correlations between pyrene degradation efficiency and the relative abundance of pyrene dioxygenase encoding genes (nidA, nidA3 and PAH-RHDα-GP). Short dash line represents the logarithmic nonlinear regression of nidA gene; long dash line represents the logarithmic nonlinear regression of nidA3 gene; dotted line represents the logarithmic nonlinear regression of PAH-RHDα-GP gene.

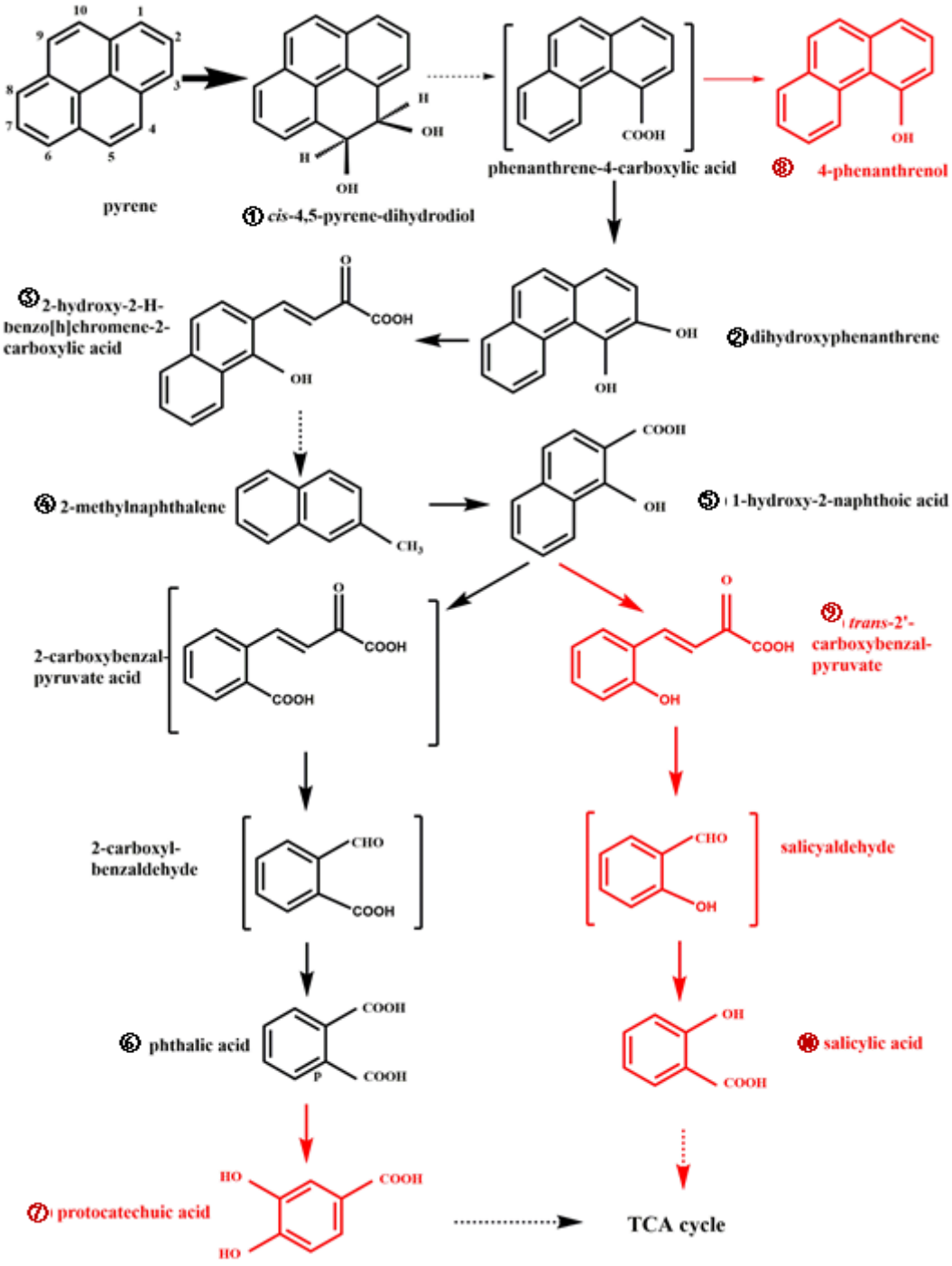

Figure 6

Pyrene degradation metabolites and pathways by the cultivable degraders Sphingomonas sp. YT1005 and MMI-enriched active pyrene degrading consortium. Dash arrows represent multiple metabolic steps. Bracketed compounds are hypothetical metabolites not identified in the present study. Compounds in black color are metabolites identified in both NC_Sph and NC_MFC treatments, following the phthalate pathway. Compounds in red color are metabolites identified only in NC_MFC treatments, following the salicylate pathway.

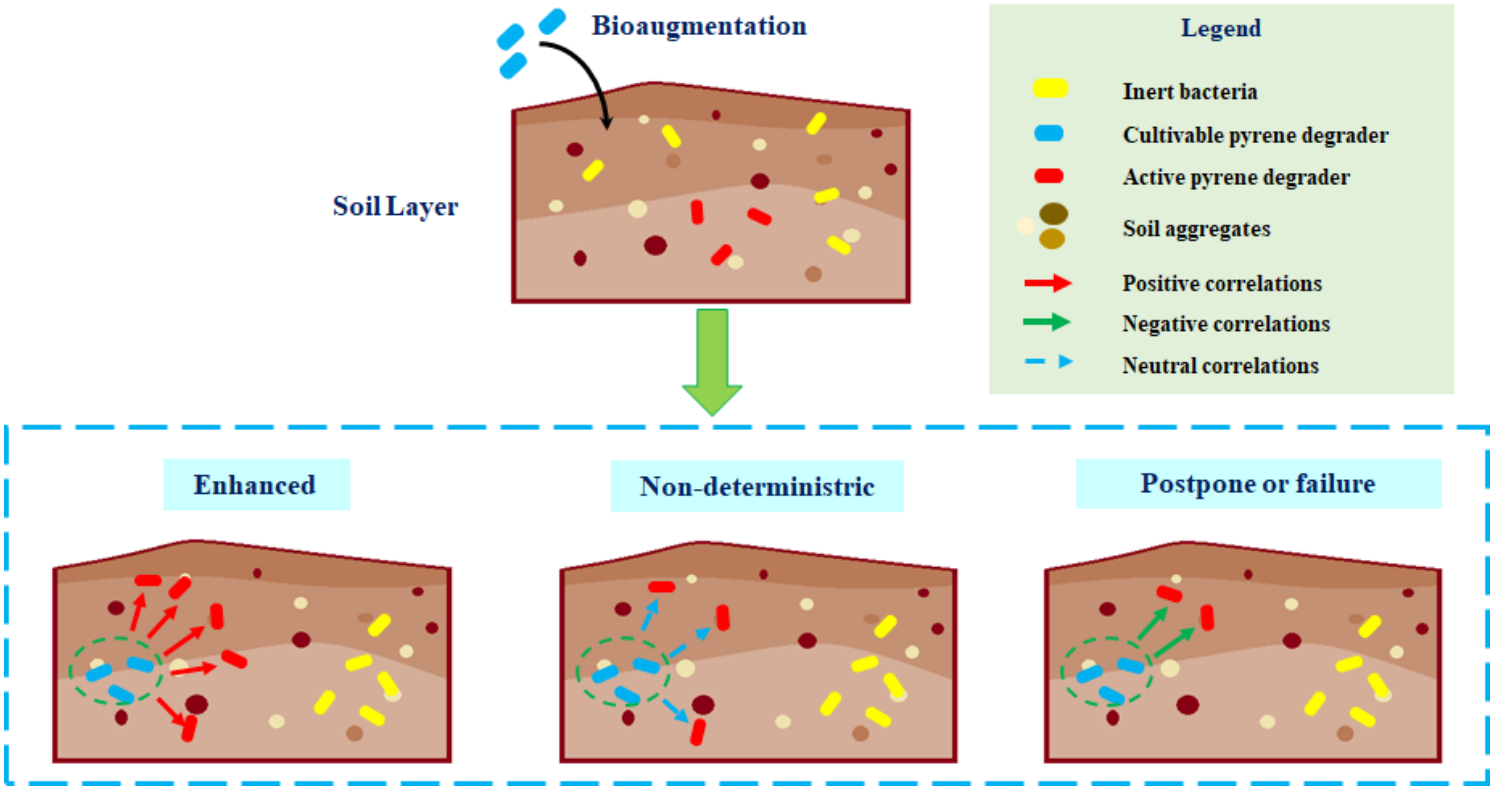

Figure 7

Schematic mechanisms of intra-correlations between the cultivable and active pyrene degraders in determining bioaugmentation performance. (A) Ehanced bioaugmentation with positive intra-correlations. (B) Non-deterministric bioaugmentation with neutral intra-correlations. (C) Bioagumentation postpone or failure with negative intra-correlations.

Supplementary Files

This is a list of supplementary files associated with this preprint. Click to download.

- SupportingInformation.docx